doi:10.3772/j.issn.1006-6748.2019.03.008

Pressure control strategy for pump motor energy transfer unit①

Yao Jing(姚 静)②[*,**,***], Zhang Wei[*], Cao Xiaoming[*], Zhao Guichun[*], Sun Menghui[**]
([*]College of Mechanical Engineering, Yanshan University, Qinhuangdao 066004, P. R. China)
([**]School of Mechanical Engineering, Nanjing Institute of Technology, Nanjing 210000, P. R. China)
([***]The Laboratory of Heavy Machinery Fluid Power Transmission and Control in Hebei, Yanshan University, Qinhuangdao 066004, P. R. China)

Abstract

Multi-level pressure source system is a novel hydraulic system with distinct advantage of energy saving. In order to balance each pressure level of the multi-level pressure source system, a pump motor energy transfer unit is usually equipped. However, the pump motor energy transfer has the characteristics of poor starting and low response, which cause long time of pressure adjustment and large pressure jitter when the transformer is switched to system suddenly and the motor-side pressure has pressure impact when rail of the pump-side is switched. To address these problems, this paper proposes a compound control strategy of feedforward compensation control with Fuzzy-PID to improve the controllability of the multi-level pressure source system. A test rig of the pump motor energy transfer unit is built and the controllability of compound controller and PID controller are compared. The experiment results show that, compared with the traditional PID, the adjustment time and the pressure impact are reduced by 20% and 25% with the proposed compound control strategy. Therefore, the presented compound control strategy can be used to improve starting performance and robustness of the pump motor energy transfer unit control system.

Key words: hydraulic system, pump-motor energy transfer unit, pressure control, energy saving

0 Introduction

For multi-actuator machines, their electro-hydraulic proportional control systems are usually dimensioned by peak pressure and peak flow rate, and have a common pressure source with one pump or multi-pump. However, the actuators generally work in part load as well as different actuators in different load conditions, which cause large throttling and overflow losses.

Lots of architectures have been proposed to improve the system efficiency. Displacement-controlled (DC) system, which is aimed at eliminating the throttling loss, has been proposed recently and demonstrated efficiency improvements in numerous prototypes of different sizes successfully. In order to achieve maximum system efficiency, a system power management method was proposed for DC hydraulic hybrid machines[1,2], but limit to its cost, it was not widely applied yet. With the development of hydraulic hybrid system, a typically architecture——STEAM was put forward[3-5], which considered the engine and hydraulic system efficiency as a whole. The hydraulic system had three constant pressure rails (HP, MP, LP), including nine force combinations. According to the cylinder load value, the pressure rail was connected selectively to match the load requirement. Each constant pressure rail had an accumulator, not only to supply the peak power, but also to realize the energy recovery. Recent research results showed that the STEAM system had a distinct advantage of energy saving, and initial field tests were very promising and showed a 39% increase in efficiency for the swing drive and a 55% increase in efficiency during air grading up compared to conventional load-sensing system in an 18 t excavator[6]. The multi-level pressure source system for improving the efficiency of hydraulic forging press was proposed based on STEAM[7]. In this system, a pump-motor energy tansfer unit (P-METU)[8,9] in coaxial series was used as the transformer to balance the energy of different pressure rails, avoiding energy excessiveness or insufficientcy of each rail. That is to say, the pressure of

① Supported by the National Natural Science Foundation of China (No. 51575471) and the Key Project of Science and Technology Plan of Higher Education of Hebei Education Department (No. ZD2017077).
② To whom correspondence should be addressed. E-mail: jyao@ysu.edu.cn
Received on Aug. 20, 2018

each rail needed to be kept at a constant value by controlling the P-METU displacement continuously, while the pressure rail connecting to the P-METU switched in or out according to the pressure value of each rail. However, the switching action could cause discrete pressure impulse to the P-METU pressure continuous control system, leading to poor starting characteristics and poor pressure control accuracy of the whole system. In order to solve this problem, the compound control strategy of the feedforward compensation control with fuzzy proportional integral derivative (PID) was proposed to improve robustness and stabilize each pressure rail rapidly for the P-METU pressure continuous control system in this study. And the proposed control strategy was tested and validated by lots of experiments.

1 Configuration and modelling

In this part, configuration of P-METU is introduced and a mathematical model of the P-METU control system is derived, which contributes to build the feedforward compensation control model.

1.1 Configuration

P-METU control system consists mainly of three constant pressure rails with accumulators (HP, MP, LP), a P-METU, six on/off valves, two pressure sensors, a rotational speed and torque sensor and a controller etc, as shown in Fig. 1. The accumulators are responsible for maintaining the rail pressure and recovering instantaneous energy. The on/off valves are used to determine which pressure rail connects to P-METU. P-METU adopts a variable displacement pump and a fixed displacement motor in coaxial. When a rail pressure is more than the set pressure (overmuch rail) and another rail pressure is lower than the set pressure (insufficient rail), the overmuch rail will be connected to the motor and the insufficient rail is always connected with the pump by switching on/off valve, and the overmuch hydraulic energy will be transferred to the insufficient rail by P-METU. In the process of energy transfer, in order to avoid that the motor-side pressure is lower than set pressure value, the close-loop control of the motor-side pressure is adopted by adjusting the variable displacement pump in real-time.

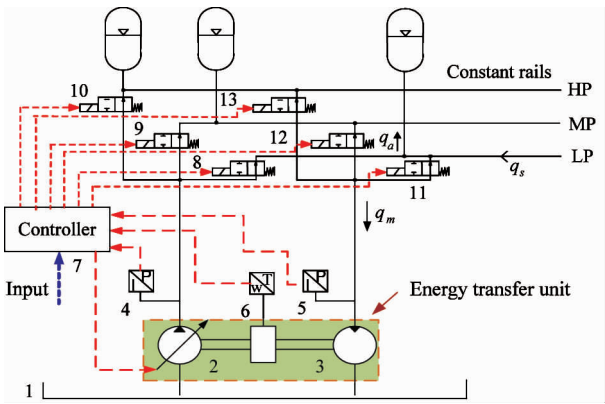

1 tank, 2 variable displacement pump, 3 motor, 4 5 pressure sensor, 6 speed and torque sensor, 7 controller, 8 9 10 11 12 13 on/off valve

Fig. 1 The P-METU control system

1.2 Mathematical model of P-METU

1.2.1 The variable displacement pump

The variable mechanism of the variable displacement pump adopts typical servo valve-controlled cylinder, its mathematical model consists mainly of servo valve model and valve-controlled cylinder model.

Considering that the variable displacement pump has a high inherent frequency, the transfer function of the servo valve can be simplified approximately to a second order oscillation link.

$$G_{sv}(S) = \frac{X_v}{i_a} = \frac{K_{sv}}{\frac{s^2}{\omega_{sv}^2} + \frac{2\zeta_0}{\omega_0}s + 1} \tag{1}$$

where, X_v is the servo valve spool displacement (m), i_a is the input current (A), K_{sv} is the servo valve spool displacement gain (m/A), ω_{sv} is the natural frequency of the servo valve (rad/s), ζ_0 is the damping ratio, ω_0 is the integrated natural frequency (rad/s).

Make k_h equal to $\frac{4\beta_e A_p^2}{V_t}$, ignoring the influence of the oil leakage and temperature variation, the valve-controlled cylinder model can be simplified as

$$x_p = \frac{\frac{K_{ps}A_p}{k_h}x_v - \frac{1}{k_h}\left(1 + \frac{V_t}{4\beta_e K_{ce}}s\right)(F_f + F_L)}{\left(\frac{s}{\omega_r} + 1\right)\left(\frac{s^2}{\omega_{sv}^2} + \frac{2\zeta_0}{\omega_0}s + 1\right)} \tag{2}$$

where, V_t is the effective control volume of hydraulic cylinder, x_p is the displacement of the variable piston (m), K_{ps} is the total pressure gain, A_p is the area of hydraulic cylinder (m^2), β_e is the bulk modulus of oil (Pa), F_f is the force of friction (N), F_l is the load (N), ω_r is the transition frequency of inertia link (rad/s).

Theoretically the displacement of the variable pump is proportional to $\tan\gamma$. Due to a small angular adjustment range ($\pm 15°$), $\frac{\tan\gamma}{\tan\gamma_{max}}$ can be considered to be equal to $\frac{\gamma}{\gamma_{max}}$, so the displacement of the variable pump can be expressed as:

$$\frac{D}{D_{\max}} = \frac{\tan\gamma}{\tan\gamma_{\max}} = \frac{\gamma}{\gamma_{\max}} = \frac{X_p}{X_{p\max}} \tag{3}$$

where, γ is the swashplate angle of the variable pump, $D_{\max}$ is the maximum displacement of the variable displacement pump (m^3/r), $\gamma_{\max}$ is the maximum swashplate inclination (rad), $X_{p\max}$ is the maximum displacement of the variable piston.

1.2.2 The fixed displacement motor

The flow continuity equation at the inlet of the motor is

$$q_m = D_m\omega + C_{tm}p_m + \frac{V_m}{\beta_e}\frac{\mathrm{d}p_m}{\mathrm{d}t} \tag{4}$$

where, D_m is the displacement of motor (m^3/r), p_m is the load pressure of motor inlet side (Pa), V_m is the The total volume of the motor and the pipe (m^3).

1.2.3 The fixed displacement motor

The torque balance equation of the mechanical shaft transmission torque is

$$p_mD_m = J\frac{\mathrm{d}\omega}{\mathrm{d}t} + B\omega + P_pD_p + T_f \tag{5}$$

where, J is the moment of inertia (kg/m^2), ω is the load pressure of motor inlet side (Pa), B is the viscous damping coefficient of pump, motor and mechanical shaft (N/(m/s)), D_p is the displacement of pump (m^3/r), P_p is the load pressure pump outlet side load pressure, T_f is the friction torque (N · m).

The open-loop control block diagram of the P-METU control system can be obtained by Eq. (1) – Eq. (5), as shown in Fig. 2.

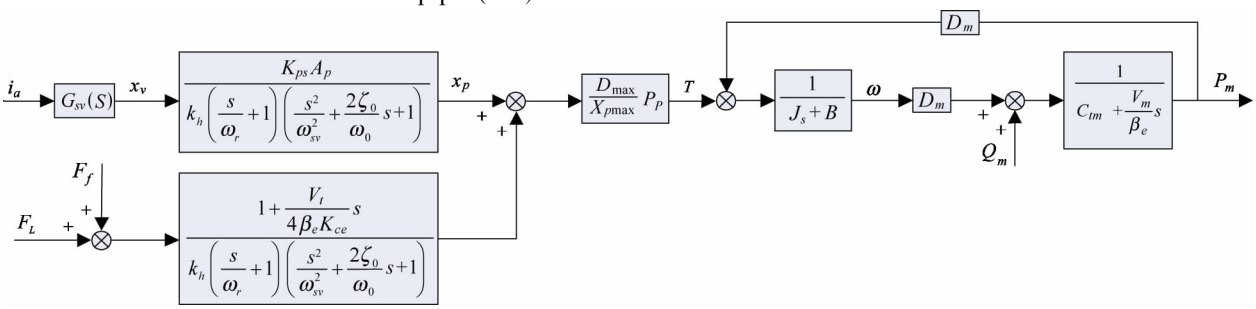

Fig. 2 Control block diagram of the P-METU control system

2 Control strategy

A feedforward compensation with Fuzzy-PID compound control strategy is investigated in this study. The feedforward compensation controller is introduced to make up for shortcomings of starting slowly and pressure jitter, and the Fuzzy-PID controller is adopted to modify the PID parameter online to improve pressure control accuracy. The system control diagram is shown in Fig. 3. In the following part, the feedforward compensation with Fuzzy-PID compound controller would be designed step by step.

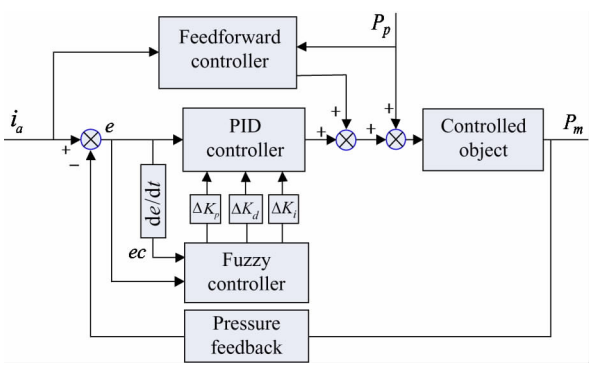

Fig. 3 The system control diagram

2.1 The variable displacement pump

The feedforward controller in this study has two types of compensation, one is input compensation, and the other is disturbance compensation, as shown in Fig. 4. Input compensation link $G_r(S)$ is used to overcome slow starting and accelerate system response. Disturbance compensation link $G_n(S)$ is used to enhance system robustness when pressure levels are switched.

According to the design approach[10], ignoring the higher order differential link, the input compensation can be expressed as

$$G_r(s) = \frac{1}{G_2(s)G_3(s)} = \frac{D_m^2 + BC_{tm}}{P_pD_mD_{\max}} \tag{6}$$

The disturbance compensation can be expressed as

$$G_n(s) = -\frac{1}{G_2(s)} = -\frac{\overline{x_{p1}}}{P_{p1}} \tag{7}$$

where, $\overline{x_{p1}}$ is the adjustment of the first stage equilibrium point, P_{p1} is the first stage of the load pressure.

2.2 Fuzzy-PID controller design

In this study, a two-dimension fuzzy controller will be used. This controller has two inputs, deviation

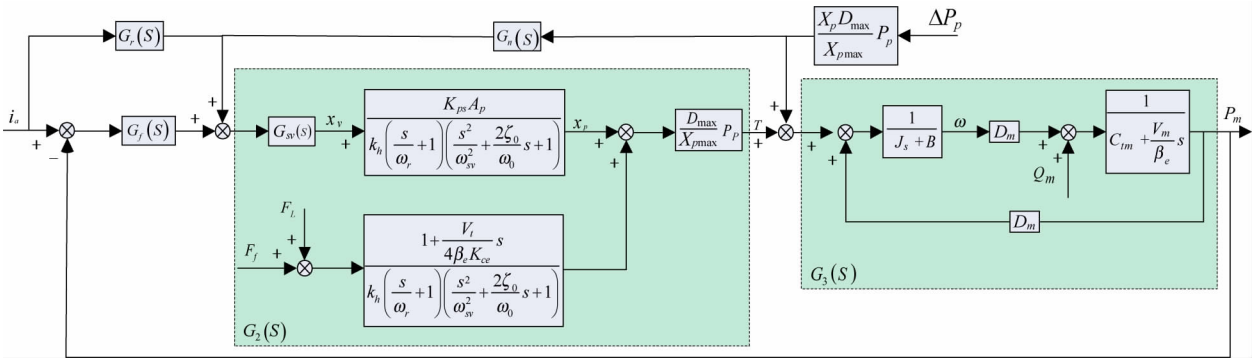

Fig. 4 P-METU feedforward-feedback compound control schematic

e and derivative of deviation ec, and three outputs, three parameters of PID controller ΔK_i, ΔK_p, ΔK_d[11,12], as shown in Fig. 3. It involves three processes: fuzzification, fuzzy control rules and defuzzification.

2.2.1 Fuzzification

In the P-METU system, the domains of input and output variables are e, ec, ΔK_p, ΔK_i, $\Delta K_d \in \{-6, -5, -4, -3, -2, -1, 0, 1, 2, 3, 4, 5, 6\}$. The relationship between the domain and the fuzzy set is obtained from the membership function curve. Combined with the actual situation, in order to reduce the complexity of the calculation, the triangular membership function is selected, as shown in Fig. 5 and Fig. 6. Signals e and ec can be divided into 7 levels of fuzzy using Gaussian membership functions with labels {NB, NM, NS, O, PS, PM, PB} in the interval $[-6, 6]$[13], as shown in Table 1.

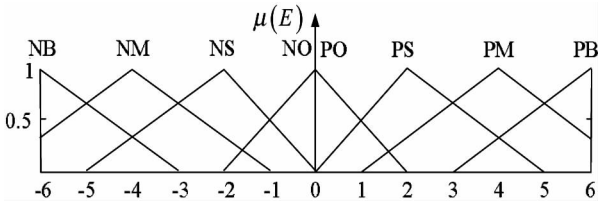

Fig. 5 Enter the membership function curve for the variable

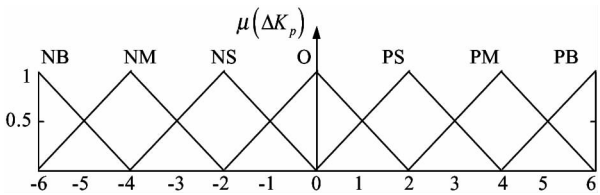

Fig. 6 The membership function curve of the output variable

Table 1 Label meanings

NB	NM	NS	O	PS	PM	PB
Negative big	Negative medium	Negative small	Zero	Positive small	Positive medium	Positive big

2.2.2 Fuzzy control rules

According to the expert's experience, the corresponding relation between e, ec and ΔK_p, ΔK_i, ΔK_d can be worked out.

1) When deviation $|E|$ is larger, it should select the larger ΔK_p to enlarge the control input, and to reduce error rapidly. However, in order to avoid derivative $|EC|$ too large instantaneously, smaller value should be selected for ΔK_d. ΔK_i is selected as zero to avoid overshoot.

2) When deviation $|E|$ and its deviation are medium-sized, ΔK_p should be selected as a smaller value. At the same time, ΔK_i and ΔK_d should be selected as the right value to ensure rapidity and eliminate steady-state error.

3) When deviation $|E|$ is smaller, ΔK_i and ΔK_p should be selected as a lager value to eliminated steady-state error and ensure rapidity. However, value ΔK_d is depended on the fluctuation range. When $|EC|$ is smaller, ΔK_d is larger, while when $|EC|$ is larger, ΔK_d is smaller.

Tables 2, 3 and 4 represent the regulation rules on parameters ΔK_p, ΔK_i, ΔK_d, respectively.

2.2.3 Defuzzification

The defuzzification process can be regarded as the inverse process of fuzzification. In the Mamdani reasoning algorithm, the default method is the centre-of-gravity method to calculate the exact value of the control output u. The calculation formula of the centre-of-gravity method can be expressed as

Table 2 Fuzzy rules of ΔK_p

$\lvert EC\rvert$	$\lvert E\rvert$							
	NB	NB	NB	NM	NM	NM	O	O
NB	NB	NB	NB	NM	NM	NM	O	O
NM	NB	NB	NB	NM	NM	NM	O	O
NS	NB	NB	NB	NM	NM	NM	O	O
O	NB	NB	NB	NM	NM	NM	O	O
PS	NB	NB	NB	NM	NM	NM	O	O
PM	NB	NB	NB	NM	NM	NM	O	O
PB	NB	NB	NB	NM	NM	NM	O	O

Table 3 Fuzzy rules of ΔK_i

$\lvert EC\rvert$	$\lvert E\rvert$							
	NB	NM	NS	NO	PO	PS	PM	PB
NB	NB	NB	NB	NM	NM	NM	O	O
NM	NB	NB	NM	NM	NS	NS	O	O
NS	NM	NM	NS	NS	O	O	PS	PS
O	NM	NS	NS	O	O	PS	PS	PM
PS	NS	NS	O	O	PS	PS	PM	PM
PM	O	O	PS	PS	PM	PM	PB	PB
PB	O	O	PS	PM	PM	PB	PB	PB

Table 4 Fuzzy rules of ΔK_d

$\lvert EC\rvert$	$\lvert E\rvert$							
	NB	NM	NS	NO	PO	PS	PM	PB
NB	PS	PS	O	O	O	O	PB	PB
NM	NS	NS	NS	NS	NS	O	PS	PM
NS	NB	NB	NM	NS	NS	O	PS	PM
O	NB	NM	NM	NS	NS	O	PS	PM
PS	NB	NM	NS	NS	NS	O	PS	PS
PM	NM	NS	NS	NS	NS	O	PS	PS
PB	O	O	PS	PM	PM	PB	PB	PB

$$u = \frac{\sum_{i=1}^{n} u(U_i)\,U_i}{\sum_{i=1}^{n} u(U_i)} \tag{8}$$

where, U_i is the controlled pressure of motor inlet side and $u(U_i)$ is the degree of membership function. At this point, a complete set of fuzzy-PID has been introduced clearly.

3 Experiment and discussion

3.1 Experiment rig

In order to validate starting, anti-interference as well as pressure control characteristic of the P-METU control system adopting feedforward compensation with Fuzzy-PID compound control strategy in this study, a P-METU control system experimental rig was built. The system schematic and the test rig are shown in Fig. 7(a) and Fig. 7(b), respectively. The test hydraulic system is able to supply HP (9 MPa), MP (7 MPa), LP(5 MPa) three pressure rails. Due to the shortage of actuators on this rig, it is hard to simulate the energy recovery and consumption at the same time, so a similar working mode is adopted. Pump 4 supplies the constant flow to motor 3 all the time to simulate the energy input, and the test focuses on whether the proposed compound control strategy can stabilize LP at 5 MPa quickly with the flow continuous input by controlling the variable displacement pump 3. Another test is to validate anti-interference of P-METU with the proposed compound control strategy. Supposing that the pressure of HP rail or MP rail is up to set point, the pump-side pressure switches suddenly between HP and LP by on/off valve 9, it is observed the pressure variation of the LP rail would have a small jitter and return to the set point quickly.

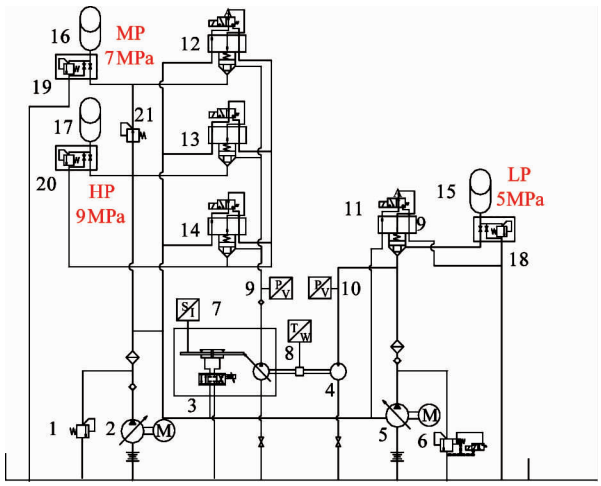

(a) Experiment schematic of the P-METU system

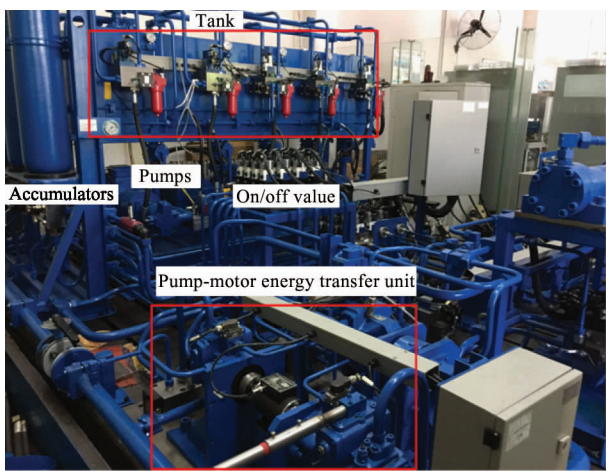

(b) The P-METU system experiment rig

Fig. 7 The P-METU control system experimental platform

The controller consists of master computer, slave computer, signal conditioner, and PCI I/O cards. Based on Matlab-Simulink software and XPC target, control system model can be compiled to generate executable code and downloaded to the slave computer. Using the I/O port, pressure signal and displacement signal can be collected and then processed by the real-time controller with sample time of 1 ms.

Main parameters of experiment rig are shown in Table 5 and Table 6.

Table 5 Sensors parameters of experiment rig

Name	Stroke	Signal	Precision
Pressure sensor	30 MPa	0 – 10 V	±0.1%
Position sensor	−25 – +25 mm	4 – 20 mA	0.5%
Rotate speed sensor	5000 r/min	4 – 20 mA	0.1%

Table 6 Sensors parameters of experiment rig

Description	Value	Description	Value
Displacement of the motor	40×10^{-6} m^3/r	Maximum displacement of cylinder	15 mm
Maximum displacement of the pump	40×10^{-6} m^3/r	Angular adjustment range of the variable displacement pump	±15 °
Frequency characteristic of servo valve	≥100 Hz	Working cylinders area	0.018 m^2
The rate flow of servo valve	20 L/min	Input compensation factor	6.89×10^{-8}

3.2 Pressure control characteristics

In order to evaluate the control strategy, the pressure control effect of PID control and the feedforward compensation control with Fuzzy-PID in the P-METU control system are studied and compared when the system starts suddenly and the load is switched frequently.

3.2.1 Starting characteristics

The pressure response curves, the motor variable mechanism displacement response curves and the P-METU rotating speed response curves with PID control and compound control are shown in Fig. 8(a), Fig. 8(b), Fig. 8(c), respectively. For the feedforward compensation control with Fuzzy-PID, when P-METU starts up, the pressure response has a 1.4 MPa pressure impact due to the pressure switching in sudden as well as PID control, which causes a step interference to the P-METU control system. After the pressure peak, due to the variable gain control, the pressure stabilizes rapidly, the fluctuation range of the pressure is obviously reduced to 0 – 0.2 MPa. The motor variable mechanism displacement rises fast without overshoot control, meanwhile the adjustment time is also reducing from 2.5 s to 0.5 s. The P-METU rotating

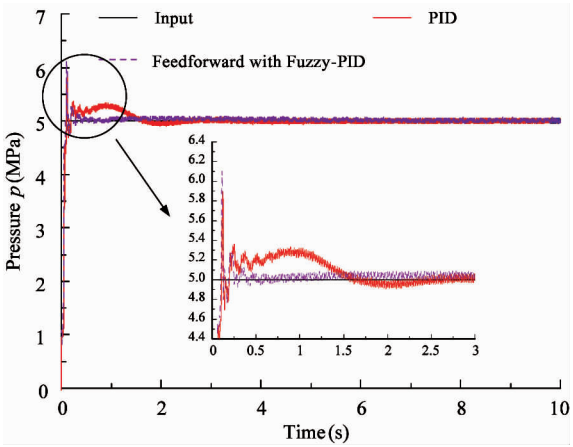

(a) Pressure response curves

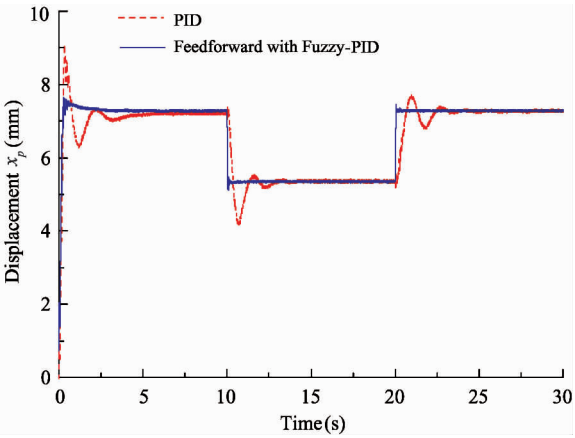

(b) Displacement response curves

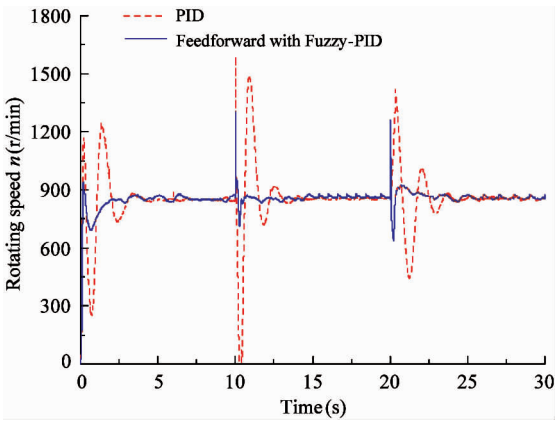

(c) Rotating speed response curves

Fig. 8 Starting characteristic curves

speed is up to set point quickly and has no large speed fluctuation compared with PID control.

3.2.2 Anti-interference characteristics

The pump-side of the P-METU control system is connected to different pressure levels through the on/off valves, and the pressure switching is simulated by opening and closing the on/off valves. The pump-side pressure switches at 10 s from 7 MPa to 9 MPa and at 20 s from 9 MPa to 7 MPa, the corresponding pressure, the displacement of the variable mechanism and the rotating speed response curves are shown in Fig. 9.

As shown in Fig. 9(a), when the pump-side pressure switching occurs, the pressure generates a 0 – 0.1 MPa jitter under feedforward compensation control with Fuzzy-PID, which accounts for 25% of that of PID control, and the pressure adjustment is completed almost within 1 s after the pump-side pressure switching. After the pump-side pressure switching, the variable mechanism reaches the steady value rapidly with the compound control. Compared with PID control, the system response becomes faster obviously after adding

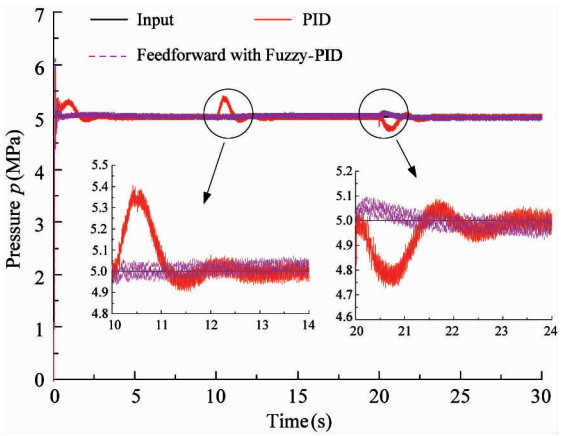

(a) Pressure response curves

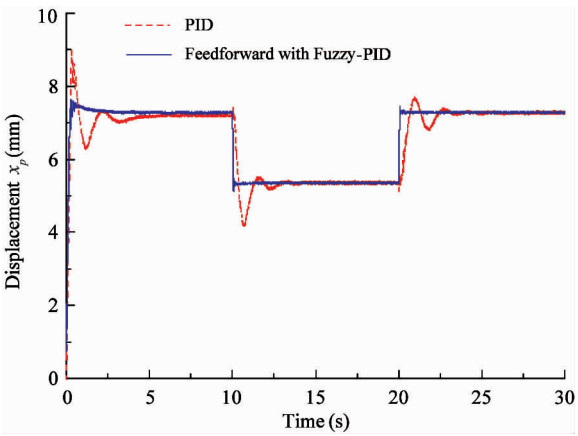

(b) Displacement response curves

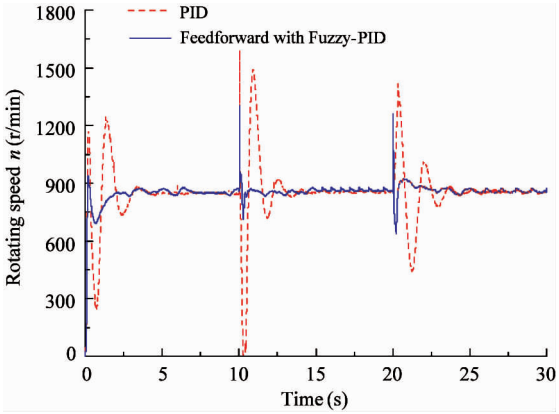

(c) Rotating speed response curves

Fig. 9 Anti-interference characteristics curves

the feedforward link. In addition, the feedforward compensation also suppresses the disturbance of the pressure switching to rotating speed, as shown in Fig. 9(c). And the fluctuation range of rotating speed reduces from 0 – 1600 r/min to 650 – 1350 r/min, so that the operation process of the system becomes more smoothly.

4 Conclusion

This study proposes a compound control strategy of the feedforward compensation control with Fuzzy-PID to improve the response and robustness of the P-METU control system. The mathematic model of P-METU is established, the feedforward compensation parameters of the controller are obtained, and the feedforward compensation control with Fuzzy-PID is designed. The starting characteristics and anti-interference characteristics are tested with the proposed compound control and PID control respectively. The experimental results show that the feedforward compensation control with Fuzzy-PID has a better response and robustness than that of PID control, and shows good performances in starting process and pressure switched process.

References

[1] Hippalgaonkar R, Ivantysynova M. Optimal power management of hydraulic hybrid mobile machines-part II: machine implementation and measurements[J]. *Journal of Dynamic Systems Measurement & Control*, 2016, 138(5), doi:10.1115/1.4032743

[2] Zimmerman J, Hippalgaonkar R, Ivantysynova M. Optimal control for the series-parallel displacement controlled hydraulic hybrid excavator[C]. In: Proceedings of the ASME 2011 Dynamic Systems and Control Conference and Bath/ASME Symposium on Fluid Power and Motion Control, Arlington, USA, 2011. 129-136

[3] Leifeld R, Vukovic M, Murrenhoff H. STEAM-the best of both worlds[C]. In: Proceedings of the 7th Workshop on Digital Fluid Power, Linz, Austria, 2015. 9-20

[4] Vukovic M, Sgro S, Murrenhoff H. STEAM-a mobile hydraulic system with engine integration[C]. In: Proceedings of the ASME/BATH 2013 Symposium on Fluid Power & Motion Control, Sarasota, USA, 2013. 231-238

[5] Murrenhaff H, Sgro S, Vukovic M. An overview of energy saving architectures for mobile applications[C]. In: Proceedings of the 9th International Fluid Power Conference, Aachen, Germary, 2014. 238-249

[6] Vukovic M, Murrenhoff S, Leifeld R. STEAM-a hydraulic hybrid architecture for excavators[C]. In: Proceedings of the 10th International Fluid Power Conference, Dresden, Germany, 2016. 151-162

[7] Yao J, Cao X, Wang P, et al. Multi-level pressure switching control and energy saving for displacement servo control system[C]. In: Proceedings of the BATH/ASME 2016 Symposium on Fluid Power and Motion Control, Bath, UK, 2016. doi: 10.1115/FPMC2016-1721

[8] Dluzik K, Aachen M C. Zylinderansteuerungen am drucknetz durch Hydro-transformatoren[J]. *Ölhydraulik und Pneumatik*, 1987(3): 248-255

[9] Dluzik K. Energiesparende schaltungskonzepte für hydrozylinder am drucknetz[J]. *Ölhydraulik und Pneumatik*, 1989 (5): 444-450

[10] Graichen, Zeitz. Feedforward control design for finite-time transition problems of nonlinear systems with input and output constraints[J]. *IEEE Transactions on Automatic Control*, 2007, 53(5):1273-1278

[11] Bo Y, Pei Z, Tang Z Y. Fuzzy-PID control of Stewart platform[C]. In: Proceedings of the International Conference on Fluid Power and Mechatronics, Beijing, China, 2011. 763-768

[12] Liu F C, Liang L H, Gao J J. Fuzzy-PID control of space manipulator for both ground alignment and space applications[J]. *International Journal of Automation and Computing*, 2014, 11(4): 353-360

[13] Jithish J, Arun N K S, Sivan D, et al. A self-tuning hybrid Fuzzy-PID controller for first order hydraulic systems [C]. In: Proceedings of the 5th International Conference on Advances in Computing and Communications, Kochi, India, 2016. 75-78

Yao Jing, born in 1978. She received the B. S. degree in Mechanical Engineering from Yanshan University, Qinhuangdao, China, in 2001, and M. S. and Ph. D degrees in Mechatronics Engineering from Yanshan University in 2004 and 2009 respectively. She is currently a professor of Mechatronics Engineering, Yanshan University, China. Her research interests include electro-hydraulic servo control and heavy machinery fluid transmission and control.